Photoemission and Photoabsorption Spectroscopy of Glycyl-Glycine in the Gas Phase

Vitaliy Feyer,*,† Oksana Plekan,†,‡ Robert Richter,† Marcello Coreno,§ Kevin C. Prince,†,∥ and Vincenzo Carravetta⊥

Sincrotrone Trieste, in Area Science Park, I-34012 Basovizza, Trieste, Italy, CNR-IMIP, Montelibretti, Rome I-00016, Italy, Laboratorio Nazionale TASC, CNR-INFM, 34012 Trieste, Italy, and CNR-Institute of Chemical Physical Processes, Via Moruzzi 1, 56124 Pisa, Italy

Received: July 20, 2009; Revised Manuscript Received: August 27, 2009

The high-resolution outer and inner valence band (VB) spectra, as well as core level X-ray photoemission (XPS) and near edge X-ray absorption fine structure (NEXAFS) spectra at the carbon, nitrogen, and oxygen K-edges of glycyl-glycine in the gas phase have been measured, and the results interpreted by means of ab initio calculations. By comparison with our previous glycine spectra, the features characteristic of the peptide bond in the carbon, nitrogen, and oxygen XPS and NEXAFS spectra of glycyl-glycine have been identified and assigned. The K-edge NEXAFS spectra at all edges were found to be in reasonable agreement with published electron energy loss spectra, but showed more prominent structure due to the higher resolution. Effects on the nitrogen K-edge NEXAFS spectrum of glycyl-glycine due to intramolecular hydrogen bonding were observed. The $N(NH_2)$ 1s $\rightarrow \pi^*_{CN}$ resonance shifts to 0.6 eV lower energy, due to internal hydrogen bonding between the NH_2 and NH groups.

1. Introduction

Recent progress in the gas phase spectroscopy of biomolecular building blocks has been driven in part by improved capabilities for studying molecules of increasing size in both experiment and theory. The gas phase experimental data serve as benchmarks for computational algorithms, while theoretical results help interpret and guide experiments.[1] Peptides and proteins are chains of amino acids held together by peptide bonds, so it is interesting to investigate the electronic structure of the molecular peptide bond. XPS probes the chemical state of a system because the binding energy shifts depend on the chemical environment of the atom that is ionized. VB and NEXAFS spectroscopy are sensitive to fine details of the electronic structure of organic molecules and give complementary information about the occupied and unoccupied valence states.

In this work we study the dipeptide glycyl-glycine (Gly-Gly), formed from two glycine (Gly) molecules (see Figure 1b). The He I valence photoemission spectra of Gly in the gas phase have been reported previously by several authors.[2−4] It is the simplest amino acid with only two carbon atoms (see Figure 1a), and has been extensively investigated both on solid surfaces with XPS,[5−9] and in solution.[10,11] As well, there are a few XPS studies of Gly in the gas phase.[12−14]

A single low resolution study has reported the changes that occur in the valence orbitals when a peptide linkage is formed in glycyl-glycine.[15] Electron energy loss spectra (EELS) of gaseous Gly and Gly-Gly have been measured by Hitchcock et al. at the carbon, nitrogen, and oxygen K-edges.[16,17] The features in the unoccupied states characteristic of the peptide bond were identified by comparison of the Gly and Gly-Gly spectra, and they include the broadening and ∼0.3 eV shift of the C 1s $\rightarrow$ π^* peak as well as a new pre-edge feature in the N 1s spectrum. The nitrogen K-edge NEXAFS spectra of aqueous Gly and Gly-Gly have also been measured as a function of pH.[10,11] In neutral solution the spectra strongly resemble the solid phase spectra, where Gly is zwitterionic, while the spectra of the basic solution resemble those of the gas phase, where Gly is not ionized. The N 1s K-edge spectrum of Gly-Gly showed a new resonance at 401.3 eV due to the N 1s $\rightarrow \pi^*_{CN}$ transition, and additionally the N 1s $\rightarrow \sigma^*_{NH}$ pre-edge transition in anionic Gly-Gly was broader than that observed in anionic Gly. The authors concluded that the peptide bond in Gly-Gly provides sufficient electron density to act as a Lewis base, and the nitrogen terminus of most proteins should exist in an acceptor-only configuration at high pH. The solid state NEXAFS spectra of Gly-Gly at the C, N, and O K-edges have been reported by Zubavichus et al. and showed features due to the formation of zwitterions ($NH_3^+CH_2CONHCH_2COO^-$) and the formation of peptide bonds. Very recent XPS measurements for C 1s, N 1s, and O 1s and ab initio Hartree−Fock calculations of Gly and Gly-Gly in the solid state have also shown that the molecules were in zwitterionic form on the Si(111)7×7 surface.[19]

To our knowledge no XPS studies of Gly-Gly in the gas phase have been reported so far. The reason for this lack of data is the difficulty of thermal evaporation of Gly-Gly, as some amino acids and peptides are very thermally sensitive and decomposition may occur.[2−4] A combination of a highly efficient experimental setup and high flux at the gas phase beamline at Elettra

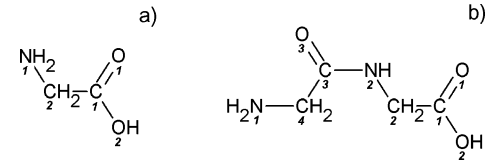

Figure 1. Schematic structures of (a) Gly and (b) Gly-Gly. Italics indicate the numbering of heavy atoms.

* To whom correspondence should be addressed. Phone: +39 0403758287. Fax: +39 0403758565. E-mail: vitaliy.feyer@elettra.trieste.it.
† Sincrotrone Trieste.
‡ Permanent address: Institute of Electron Physics, 88017 Uzhgorod, Ukraine.
§ CNR-IMIP.
∥ Laboratorio Nazionale TASC.
⊥ CNR-Institute of Chemical Physical Processes.

10.1021/jp906843j CCC: $40.75
Published on Web 09/16/2009

allowed us to obtain high-quality data, without thermal decomposition.

2. Experimental and Theoretical Methods

The measurements were carried out at the gas phase photoemission beamline, Elettra, Trieste,[20] using a 6-channel, 150 mm hemispherical electron energy analyzer mounted at 54.7° with respect to the electric vector of the light.

The Gly-Gly sample supplied by Sigma Aldrich in the form of crystalline powder with minimum purity of 99% was used without further purification and sublimated from a noncommercial, noninductively wound furnace, equipped with a chromel/alumel thermocouple. The evaporation temperature was 405 K, and the pressure in the chamber remained in the low 10^{-8} mbar range during the experiments. The experimental details are described in ref 14.

The photoemission spectra were measured with a total resolution (photon + analyzer) of 0.2, 0.57, 0.59, and 0.78 eV at $h\nu = 99$ (VB), 382 (C 1s), 495 (N 1s), and 628 eV (O 1s), respectively. The energy scale of the valence band spectrum was calibrated by using the Ne 2p and H_2O (from residual gas) valence spectra,[21] while for XPS, the spectra were referred to the following core levels and gases: 297.6 eV (C 1s, CO_2);[22] 409.9 eV (N 1s, N_2);[23] and 541.3 eV (O 1s, CO_2).[23,24] The resolution was checked by measuring photoemission from the core levels of these reference samples.

The NEXAFS spectra were recorded by collecting the ion yield signal with a channel electron multiplier placed close to the ionization region, and they were normalized to the photon flux measured by a photodiode. In this geometry, some energetic ions may be lost, so the ion yield is partial rather than total. The energy scales of the spectra were calibrated by taking simultaneous spectra of the samples and a calibrant gas introduced into the experimental chamber. The energies of the peaks of the calibrating gases were the following: 290.77 eV (C 1s $\rightarrow \pi$, CO_2);[25] 400.87 eV (N 1s $\rightarrow \pi$, N_2);[26] and 535.4 eV (O 1s $\rightarrow \pi$, CO_2).[27] The NEXAFS spectra were recorded with energy resolution of 0.07, 0.06, and 0.10 eV at the C, N, and O K-edges, respectively.

The XPS spectrum was computed by ΔSCF calculations of the core ionization potential at each C, N, and O site, at the geometry of the ground state optimized as discussed in the following, using the DALTON package[28] and the Ahlrichs[29] basis set {C,N,O(10s,6p) $\rightarrow$ [6s,3p], H(4s) $\rightarrow$ [2s]}. This basis set was augmented with {5s, 5p, 5d} diffuse functions on the site of ionization/excitation, for a better description of the lowest virtual orbitals in the NEXAFS spectrum calculation. The same photoemission intensity for each ionization process was assumed, which is a good assumption owing to the high photon energy. This approach neglects the effect of the electron correlation, assumed almost constant for the ionization of nonequivalent atoms of the same kind, but includes the electronic relaxation that is the major effect in core ionization and may significantly affect the chemical shift. The photoabsorption spectrum was, instead, computed by the STEX method extensively described elsewhere;[30] its merits and limits when applied to the simulation of the NEXAFS spectra of glycine have been discussed in detail in our previous paper.[31]

Before the experiment, we checked the purity of the sample and absence of thermal decomposition, and determined the appropriate temperature for evaporation offline in another apparatus, using photoionization mass spectrometry. During the photoemission experiment the sample quality was monitored by valence band photoemission, and no signs of thermal decomposition were observed (for example, time dependent changes, presence of decomposition products such as water or carbon dioxide, change of color of the sample after the experiment, etc). Extreme care was necessary for optimizing the evaporation conditions as only slightly elevated temperature led to thermal decomposition over the time necessary to carry out the experiment.

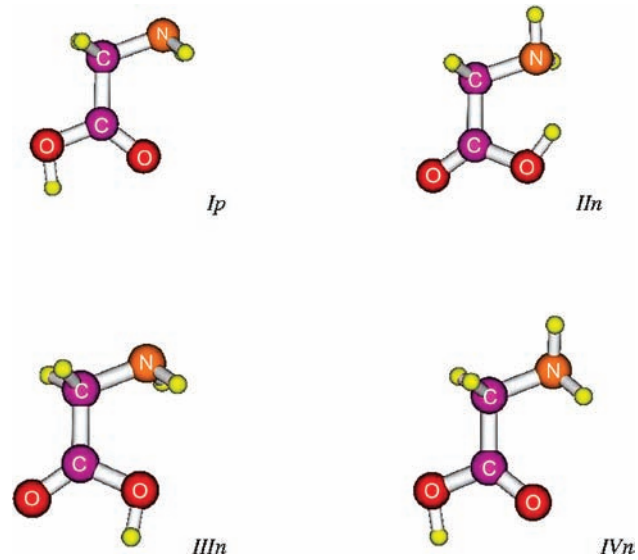

Figure 2. Most stable gas phase conformers of glycine labeled following the nomenclature proposed by Csaszar[33] where *p* and *n* indicate that the heavy atoms are coplanar or noncoplanar, respectively.

3. Results and Discussion

3.1. Geometry Optimization of Gly and Gly-Gly Conformers. Amino acids and their peptides generally exist at laboratory temperatures as several conformers of comparable energy, and the determination of their properties is a challenge of fundamental importance. Glycine conformers in the gas phase have been extensively studied by both experimental and theoretical investigations. The recent paper[32] reports new accurate density functional theory (DFT) and Møller−Plesset second order perturbation theory (MP2) calculations together with an extended comparison with most previous theoretical work. There is a general consensus that the most stable conformational structure is the one labeled *Ip*,[33] reported in Figure 2. It is a structure with the heavy atoms in the same plane and two hydrogen bonds between the amino hydrogens and the carbonyl oxygen. The following structures do not have the heavy atoms in the same plane and their stability order remains controversial; that presented in Figure 2 is the order suggested by the recent calculations.[32] As stressed by Ke et al.,[32] a quantitative understanding of relative conformer stabilities requires the inclusion of thermal vibrational contributions, as well as the zero point energy (ZPE) term, and the calculation of ΔG. By adopting the values computed in ref 32 for ΔG_{298K} the following relative populations of the four conformers in Figure 2 can be obtained: *Ip*(1.00), *IIn*(0.16), *IIIn*(0.15), and *IVn*(0.09).

Fewer conformational studies for Gly-Gly molecules are available in the literature [ref 34 and references therein]. The DFT and coupled cluster (CCSD(T)) calculations[34] show that the conformers of Gly-Gly with the lowest relative energies have the structures reported in Figure 3. Each Gly-Gly conformer is stabilized by the presence in its structure of a number (two at

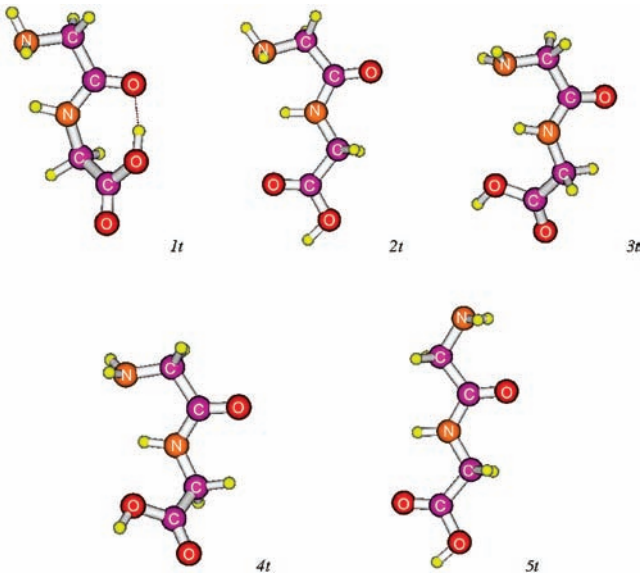

Figure 3. Gas phase conformers of Gly-Gly with the lowest relative energies, labeled according to the nomenclature proposed in ref 32 where *t* indicates a trans structure.

least) of intramolecular hydrogen bonds of different length and strength, the shortest one being that indicated by a dotted line in the *1t* structure. It may be argued that, as was discussed for glycine conformers, relative free energy should be considered for a better estimation of the conformational stability. In ref 32 the relative energy and ZPE have been reported and it was shown that the structure *2t* of Gly-Gly is the most stable one. We computed relative free energy, ΔG, at the experimental temperature $T = 405$ K, for the five structures reported in Figure 3. Both geometry optimization and vibrational analysis were performed at the DFT level by employing GAMESS[35] with the B3LYP density functional and the TZV basis set (C[5s,3p],H[3s]). By using computed ΔG_{405K} values, the relative populations of the five conformers in Figure 3 have been estimated as follows: *1t*(0.09), *2t*(1.00), *3t*(0.03), *4t*(0.01), and *5t*(0.01). It was concluded that, also at this level of theory, the conformer *2t* is the most stable one and much more populated than the other four conformers considered at the temperature of the present measurements.

3.2. Valence Photoemission Spectra. The valence photoemission spectrum of Gly-Gly measured at photon energy 99 eV is shown in Figure 4, and is better resolved than a previously reported He I spectrum.[15] The binding energies (BE) and assignments of the spectral features are presented in Table 1. For comparison the valence spectrum of Gly is also presented in Figure 4, measured under the same experimental conditions. As the gas density is not known precisely, it is not possible to normalize the intensity to the molecular density, so we use an alternative approach. Since the bonding is generally similar in the two compounds, we expect the molecular orbitals to have similar photoionization cross sections, and the number of orbitals is proportional to the number of valence electrons. Thus the integral intensities of the spectra (see Figure 4) were normalized to the total number of outer and inner valence electron in the two molecules, counting 1 electron for H atoms and 4, 5, and 6 electrons for C, N, and O atoms, respectively. This approximate normalization facilitates the interpretation of the spectra in terms of whether peaks have increased or decreased in intensity, or shifted in energy.

The first symmetric peak in the valence photoemission spectra of Gly at BE 10 eV corresponds to the ionization of the N lone-pair orbital (n_N),[2−4] while the first band in the Gly-Gly spectrum consists of two features, a peak *a* at 9.65 eV and a shoulder *b* at 10.05 eV of BE. If the first peaks of Gly-Gly (including the shoulder *b*) and Gly are integrated, the ratio of intensity is about 2.6 to 2.7 (depending on integration method), which indicates that there are probably three molecular orbitals contained in the first feature of Gly-Gly, rather than two suggested by the peak and its shoulder *b*.

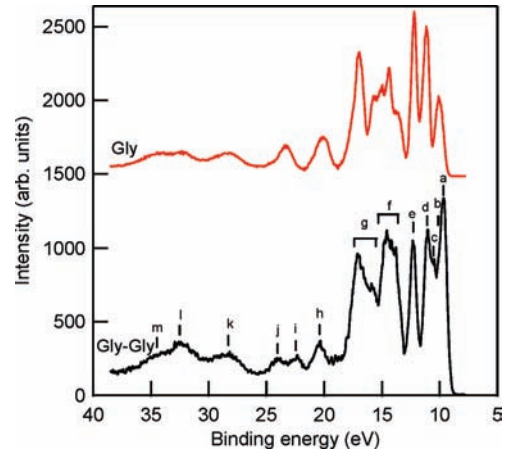

Figure 4. Valence band photoemission spectra of Gly (top curve, red)[14] and Gly-Gly (bottom curve, black) at photon energy 99 eV.

TABLE 1: Valence Band Energies and Proposed Assignments for Gly-Gly

spectral features	binding energy (eV), ±0.1 eV	assignments
a	9.65	n_N
b	10.05	n_O (peptide)
c	10.6	π_2 (peptide)
d	11.0	n_O (nonbonding)
e	12.3	π_{OO}, π_1
f	13.0−15.5	σ
g	15.5−19.0	σ
h	20.4	C 2s
i	22.45	C 2s
j	24.05	C 2s
k	28.3	N 2s
l	32.3	O 2s
m	34.3	O 2s

The next prominent feature *c* in the Gly-Gly spectrum appears at 10.6 eV and a peak *d* at 11.0 eV is present. The single nonbonding O orbital (n_O) in the glycine spectrum, which is localized on the oxygen atom of the carbonyl group, was previously observed at 11.2 eV.[4] As proposed by Richer et al.,[15] we expect to have two low-energy peaks due to the CONH group, and furthermore in amides the n_O and higher π_2 orbitals are close to one another, and within half an electronvolt in all known cases. Following Richer, we assign the peaks at 9.65 and 11.0 in the Gly-Gly spectrum, as for Gly, to the lone-pair n_N and nonbonding n_O orbitals, and the new shoulders at 10.05 and 10.6 eV to the ionization of n_O and π_2 orbitals in the peptide group. Another π_{OO} orbital on the carboxylic group in the Gly valence spectrum was observed at 12.2 eV (see Figure 4). The corresponding peak *e* in the Gly-Gly spectrum is observed at 0.1 eV higher energy and is distinctly broader, probably due to the overlapping π_1 orbital of the peptide bond[15] and π_{OO} of the carboxylic acid group.

The broad bands *f* and *g* in the valence band spectrum of Gly-Gly between 13.0−15.5 eV and 15.5−19.0 eV (see Figure 4) can be assigned to ionization of several σ-type orbitals formed by the 2p orbital of C, N, and O atoms.[36] They show a different

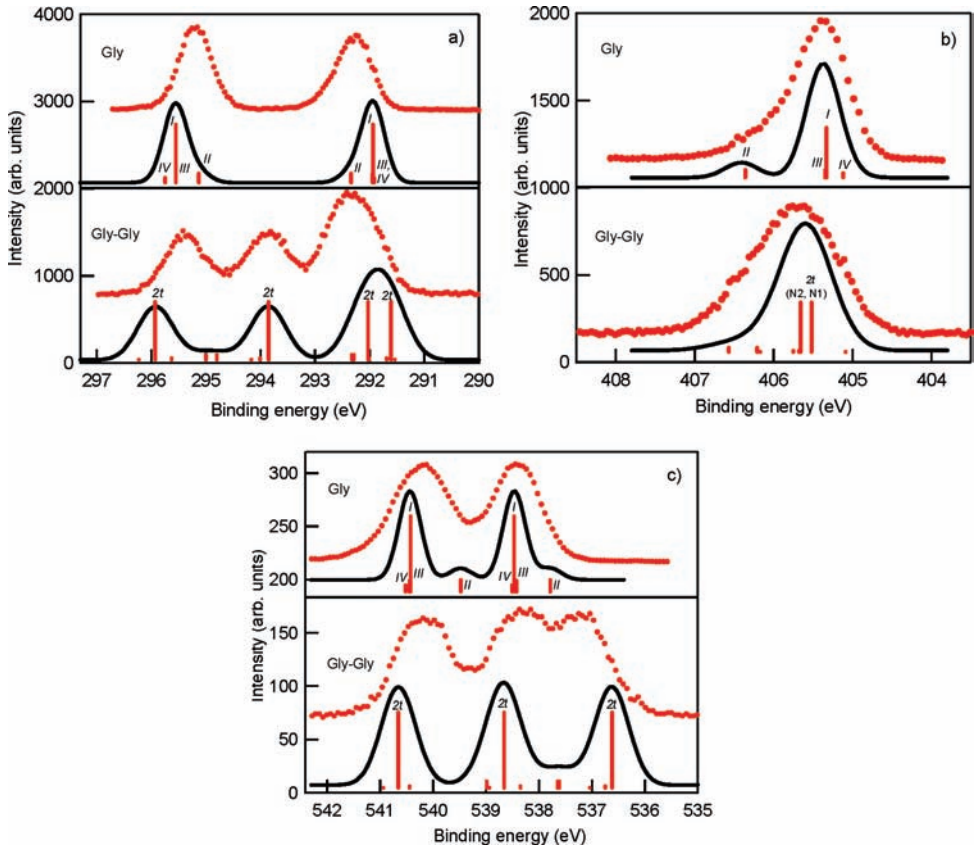

Figure 5. Core level spectra of Gly[14] and Gly-Gly, points: (a) carbon 1s, (b) nitrogen 1s, and (c) oxygen 1s. The bar height is proportional to the calculated population of the conformers. Full lines were obtained by convolution of the theoretically calculated spectrum with a Gaussian function of fwhm = 0.5 and 0.75 eV for Gly and Gly-Gly, respectively. The computed C 1s, N1s, and O 1s spectra are shifted by −1.15, −0.2, and 0.35 eV, respectively.

intensity ratio compared with the Gly spectrum, as well as an additional feature at ∼16.2 eV, where the Gly spectrum showed a deep minimum. The three peaks (*h*−*j*) centered at 20.4, 22.45, and 24.05 eV have mostly C 2s character, and in contrast the Gly spectrum shows only two peaks at 20.2 and 23.3 eV in this BE region. The peak *k* in the VB spectrum of Gly-Gly associated with N 2s is centered at ∼28.3 eV and *l* and *m* with O 2s ionization appear at ∼32.3 and ∼34.3 eV (Figure 4), and are very broad. The BEs of these orbitals are similar to those observed in the Gly spectrum.[14]

3.3. Core Level Photoemission. In Figure 5 the carbon, nitrogen, and oxygen 1s spectra of Gly-Gly are compared with those of Gly,[14] and the computed core level spectra for individual conformers are shown as bars, whose height indicates relative intensity proportional to relative population of conformers, assuming similar photoionization cross sections for chemically shifted ionization sites. The figure also shows the theoretically calculated intensities convoluted with a Gaussian function of constant full width at half-maximum (fwhm) of 0.5 (Gly) and 0.75 (Gly-Gly) eV to simulate the vibrational bandwidth and the experimental resolution. The experimental and theoretical BEs, and experimental fwhms, are summarized in Table 2.

The C 1s spectrum of Gly-Gly shows three peaks with intensity ratios of 1:1:2 (Figure 5a), and as for Gly,[12,14] the peak at 295.37 eV (295.2 eV for Gly) is assigned to the carboxylic carbon atom (C1) and the peak at 292.32 eV to the amino bonded C2 and C4 atoms. The C1 derived peak is not only slightly shifted but also broader than in Gly. The C2/C4 peak is also broader (fwhm ≈ 1.1 eV) compared with the feature due to C2 in the Gly spectrum (fwhm ≈ 0.77 eV, see Table 2 and ref 14). The broadening is mainly due to the small difference in binding energies for C2 and C4, Table 2, as well as the Franck−Condon envelope. The presence of molecular conformers is less likely to have an effect on the shapes of C 1s photoionization spectra (as observed for ethanol,[37] butyronitrile, 1-fluoropropane, and propanal[38]) because our calculations show that a single conformer, *2t* Gly-Gly, is dominant.

The peak in the Gly-Gly spectrum at 293.85 eV, which was not observed in the C 1s spectrum of Gly, is assigned to the C3 carbon atom in the peptide group, and is well reproduced by theory. The C 1s XPS spectrum of Gly-Gly was measured at photon energy ∼90 eV above threshold where the cross section does not change significantly for different carbon atoms, and under these experimental conditions the photoemission spectrum is quantitative, and indeed the intensity ratios of the peaks in the C 1s spectrum of Gly-Gly agree with the values predicted from stoichiometry within 1% (see Table 2 and Figure 5a). The C 1s spectrum of solid state Gly-Gly[19] showed a two-peak structure with a prominent shoulder at lower BE, and lower BE features were assigned to the C2 and C4, while the peak at higher BE corresponded to the deprotonated carboxylic (−COO^-) and amide (−CONH−) carbons. Gly-Gly in the solid state exists in zwitterionic form, so spectral differences are expected with respect to neutral Gly-Gly. Deprotonation of the carboxylic acid group may be expected to shift the C1 binding energy to lower values, so that it overlaps C3. Thus these results are consistent with our results for the neutral molecule.

The N 1s spectra of Gly-Gly and Gly are shown in Figure 5b, and the Gly-Gly spectrum is significantly broader (fwhm ≈ 1.3 eV) than that of Gly (fwhm ≈ 0.89 eV).[14] Although it contains contributions from both the amino (N1) and peptide nitrogen atoms (N2), the calculated difference in binding energy

TABLE 2: C 1s, N 1s, and O 1s Calculated and Measured Binding Energy (eV) for Different Conformers of Gly-Gly and Gly[a]

		conformers								
molecule	core level	*1t*	*2t*	*3t*	*4t*	*5t*	experiment (eV)	fwhm (eV), Gaussian fit	assignments	area
Gly-Gly	C 1s	293.44	293.18	293.16	293.16	293.47	292.32	1.10	C2	1.98
		293.48	292.76	292.84	292.84	292.69			C4	
		295.95	295.00	295.16	295.16	295.32	293.85	0.94	C3	1.00
		296.15	297.08	296.78	296.78	297.38	295.37	0.94	C1	0.99
	N 1s	406.41	405.72	405.88	405.88	405.29	405.70	1.3	N1	
		406.77	405.86	405.95	405.95	406.37			N2	
	O 1s	537.27	536.27	536.40	536.40	536.69	537.15	1.18	O3	0.97
		537.30	538.31	538.00	538.00	538.59	538.40	1.15	O1	0.97
		538.64	540.31	540.10	540.10	540.59	540.17	1.20	O2	1.00

		conformers							
molecule	core level	*Ip*	*IIn*	*IIIn*	*IVn*	experiment (eV)[14]	fwhm of the Gaussian fit function (eV)[14]	assignments[14]	area[14]
Gly	C 1s	293.09	293.49	293.10	293.07	292.3	0.77	C2	0.96
		296.70	296.28	296.70	296.90	295.2	0.71	C1	1
	N 1s	405.58	406.61	405.60	405.37	405.4	0.89	N1	
	O 1s	538.12	537.44	538.07	538.16	538.4	1.07	O1	1
		540.08	539.13	540.10	540.17	540.2	1.44	O2	0.79

[a] The numbering of atoms corresponds to that reported in Figure 1 containing the schematic structures of the molecules in Figures 2 and 3.

is only ~0.14 eV (Table 2), so this is not the major cause of the increased width. Also conformers are unlikely to be responsible, as the populations of conformers other than *2t* are very small, and do not significantly influence the theoretical line shape. A possible cause of the increased broadening is the larger number of vibrational degrees of freedom which could lead to different Franck−Condon envelopes for the two nitrogen atoms in Gly-Gly.

The asymmetric shape of the N 1s spectrum of Gly, particularly the tail at higher binding energy, is assigned to contributions of the different molecular conformations of the molecules (see Figure 5b). The OH···N hydrogen bond in the *IIn* conformer shifts the N 1s core level to ~1.0 eV higher binding energy (see Figure 5b, Table 2.). However, due to the low population of this conformer the feature at higher binding energy is less prominent in the spectrum than for previously studied amino acids.[13,14,39,40] Another type of hydrogen bond OH···O which exists in the peptide (*1t* conformer in Gly-Gly) shifts the N 1s core level by ~0.7−0.5 eV to higher binding energy (see Figure 5b, Table 2b), but the population is too low to influence the experimental spectrum.

The published N 1s core level spectrum of Gly-Gly in the solid state shows two peaks separated by 1.5 eV, and the lower BE feature was assigned to the peptide nitrogen 1s, and the peak at higher BE to the protonated amino nitrogen of zwitterionic Gly-Gly.[19] In this case the zwitterionic state in the condensed phase splits the overlapping nitrogen peaks.

The computed and measured O 1s core level spectra of Gly-Gly are displayed in Figure 5c, and the binding energies are summarized in Table 2. The two higher BE peaks in the Gly-Gly spectrum are located at similar BE to those of Gly, and are assigned accordingly,[12,14] namely the oxo oxygen (O1) gives rise to the peak at 538.40 eV, and the hydroxy (O2) atom to the peak at 540.17 eV. The additional peak centered at 537.15 eV corresponds to the ionization of the 1s electron of the oxo oxygen atom (O3) bonded to carbon C3 (see Figure 1b), which has a chemical shift of 1.25 eV compared with the oxo oxygen atom O1 located in the carboxylic group.

Theoretically we predict an energy shift of ~1.0 eV in the O 1s spectra of different conformers because of the OH···N and OH···O hydrogen bonds in Gly and in Gly-Gly, respectively (see Table 2). However, experimentally we have not observed clear evidence of features deriving from different conformers due to the limitations of experimental resolution, broad natural widths, and the Franck−Condon envelope.

3.4. C, N, and O K-Edge NEXAFS Spectra. Figure 6 presents the C, N, and O 1s NEXAFS spectra of Gly-Gly and calculated spectra for the conformer *2t*. The bars are proportional to the oscillator strengths and correspond to the energies and intensities computed by the STEX method; the full line is the sum of the channel cross sections obtained by Stieltjes imaging (SI) above the channel ionization threshold and convoluted with a Gaussian function (fwhm = 0.7 eV). We find very good agreement between the experimental and calculated spectra.

The C K-edge NEXAFS spectrum of Gly-Gly is shown in Figure 6a, including the spectrum of Gly (inset) for comparison, and the data and assignments are summarized in Table 3. The Gly-Gly spectrum shows a strong asymmetric peak with a maximum at 288.4 eV of width 0.9 eV, and a shoulder at a lower energy of 288.18 eV. We assign the main structure (as for Gly) to the excitation of the carboxylic carbon C1 1s → $\pi^*_{C=O}$ resonance.[31] The feature at 288.18 eV is assigned to the C3 1s → $\pi^*_{C=O}$ transition in the peptide moiety. Although these two features were not resolved in the π^* region of the published EELS spectrum of Gly-Gly, the authors predicted from calculations two resonances at 288.26 and 288.6 eV due to the excitation of 1s electrons of C3 and C1, respectively,[16,17] which is in agreement with our observation. The assignments are also supported by previous EELS studies of formamide ($HCONH_2$) and formic acid (HCOOH),[41] where the $\pi^*_{C=O}$ resonance in the C 1s spectrum for formamide appeared at lower energy than in the formic acid spectrum. Our assignments are consistent with the results of Zubavichus et al.[18] for thin films of Gly, Gly-Gly, and triglycine. Without solid state effects we are able to resolve finer structure.

Theory predicts a small shoulder on the Gly-Gly main peak at lower energy (~287.8 eV) related to the σ^*_{CH} resonance and with some Rydberg character; however, it appears to be unresolved from the main peak experimentally. The weak peak at 289.75 eV is due to the transitions of C2 and C4 1s → σ^*_{CN} and 3p Rydberg states.[16,31] On the basis of previous studies of Gly and Gly-Gly in the gas phase[16,31] and in the solid phase[18,42,43]

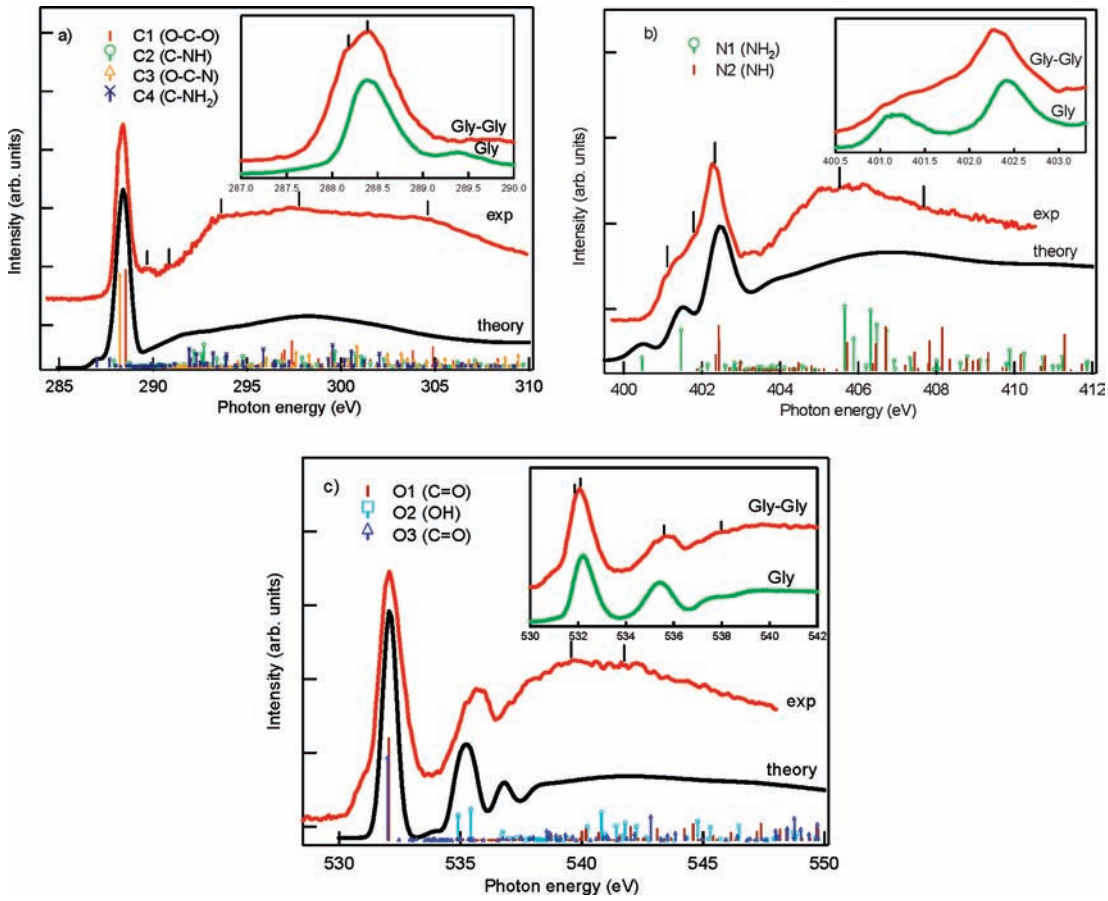

Figure 6. NEXAFS spectra of Gly-Gly: (a) C K-edge, (b) N K-edge, and (c) O K-edge. The bars indicate the calculated energies and intensities of the resonances of conformer *2t* of Gly-Gly. The lower curve is the broadened sum. The computed C K-edge, N K-edge, and O K-edge spectra are shifted by −2.5, −1.45, and −1.3 eV, respectively. Insets: Enlargement of the first part of each spectrum compared with Gly.[29]

TABLE 3: Energies of X-ray Absorption Peaks and Assignments at the C 1s, N 1s, and O 1s Edges

K-edges	energy (eV)	term value (eV)	theoretical value[a] (eV)	oscillator strengths	assignment	literature values[16,17] (eV)
C 1s			287.02	0.0063	C4 1s → σ^*_{CH} + Rydberg	
			287.69	0.0059		
			287.92	0.0046	C2 1s → σ^*_{CH} + Rydberg	
			287.98	0.0010		
	288.18	5.67	288.25	0.0697	C3 1s → $\pi^*_{C=O}$	288.26
	288.40	6.97	288.55	0.0735	C1 1s → $\pi^*_{C=O}$	288.6
	289.75	2.57	288.61	0.0011	3p Rydberg	289.7
			288.75	0.0013	C4 1s → σ^*_{CN}	
			288.64	0.0027	3p Rydberg	
			288.8	0.0028	C2 1s → σ^*_{CN}	
	290.80	1.52			C2, C4 1s → σ^*_{CH}, σ^*_{NH}	291.0
	293.70				C2, C4 1s → σ^*_{CC}, C1 1s → σ^*_{OH}	
	297.80				C1 1s → $\sigma^*_{C=O}$, shape resonance	298.0
	304.80				shape resonance	303.0
N 1s	401.1	4.4	400.48	0.0021	N1 1s → σ^*_{NH} + 3p Rydberg	401.0
	401.80	3.9	401.48	0.0067	N1 1s → π^*_{CN}	402.8
	402.30	3.4	402.37	0.0025	N2 1s → σ^*_{NH} + 3p Rydberg	401.9
			402.44	0.0073	N2 1s → π^*_{CN}	
			402.45	0.0050		
	405.70	0			N1 1s → σ^*_{NC}, σ^*_{NH}	405.7
	407.35				N2 1s → σ^*_{NC}	408.6
O 1s	531.85	5.3	532.04	0.0260	O3 1s → $\pi^*_{C=O}$	531.9
	532.20	6.2	532.08	0.0319	O1 1s → $\pi^*_{C=O}$	532.2
	535.40	4.77	534.93	0.0079	O2 1s → 3s/σ^*_{OC}	534.0
			535.45	0.0097	O2 1s → π^*_{OC}	535.7
	537.1	2.67	536.74	0.0016	O2 1s → 3p	
			536.75	0.0025	O2 1s → σ^*	
	539.5	0.67			O2 1s → σ^*_{OH}	539.0
	542.5				O2 1s → σ^*_{C-OH}	542.0

[a] The calculated values of resonances at C K-edge, N K-edge, and O K-edge have been shifted by −2.5, −1.45, and −1.3 eV, respectively, to align the experimental energies.

by NEXAFS and EELS spectroscopy, the features at 290.8, 293.7, and 297.8 eV are assigned to the excitation of C 1s → σ orbitals, see Table 3.

The N K-edge NEXAFS spectra of Gly-Gly and Gly are presented in Figure 6b, and energies of the resonances and proposed assignments are summarized in Table 3. In our recent studies[31] of Gly in the gas phase the strong resonances at ~401.2 and 402.4 eV were assigned to N1 1s → σ^*_{NH} and N1 1s → π^*_{CN} transitions, respectively. Previously Gordon et al. and Cooper et al. attributed these features in EELS spectra of both species (Gly and Gly-Gly) mainly to N1 1s → 3s, 3p Rydberg states.[16,17] The assignments were based on the fact that in the spectrum of solid Gly, no peaks in the 401−403 eV energy range were present, which is consistent with the idea that Rydberg transitions were quenched in the solid state. However, Zubavichus et al. measured N K-edge NEXAFS spectra of Gly in the solid phase and the strong peak at 401.5 eV was assigned to the N1 1s → σ^*_{NH} transitions, that is, to antibonding molecular orbitals with N−H character. Our assignment for Gly is also in agreement with NEXAFS studies of aqueous Gly measured by Messer et al.[10] They found that at low and moderate pH, where both Gly and Gly-Gly are zwitterions, the N K-edge NEXAFS spectra were nearly identical with the solid phase spectrum, where no features in the 401−403 eV energy range were observed. However, in basic solution, where the Gly and Gly-Gly are in an anionic form, they resembled the gas phase spectrum with prominent peaks in the same energy range. On the basis of experiment and theoretical calculation, they assigned the structures at 401.3 and 402.5 eV in their spectra of Gly and Gly-Gly in basic solution to 1s → σ^* transitions, and showed that these transitions in zwitterionic species shifted to higher energy and overlapped with the main peak due to the σ^* resonance at ~406 eV, which explained the difference observed by Gordon et al.[16] in the gas phase and the solid state spectra of Gly. The recent result by Otero and Urquhart[44] confirmed that condensed molecules that contain the unprotonated amine group ($-NH_2$) showed a distinct low-energy band at 402.3−402.5 eV due to the σ^*_{NH} resonance in their N 1s NEXAFS spectra, while for species with a protonated amine group ($-NH_3^+$) this feature was shifted to the higher energy of 406.0−406.8 eV.

The main difference between Gly and Gly-Gly spectra is observed in the region (~401.8 eV) where the Gly spectrum shows a minimum (see Figure 6b), while Gly-Gly manifests intensity. Our calculation shows that due to the internal hydrogen bonding between the NH_2 and NH groups in the *2t* conformer, the resonance associated with N1 1s → π^*_{CN} transition shifts to ~0.6 eV lower energy with respect to Gly, and appears at 401.8 eV, while the resonances related to the peptide nitrogen atom N2 1s → π^*_{CN}, σ^*_{NH} contribute to the sharp peak at ~402.3 eV. This assignment is in disagreement with previous EELS of Gly-Gly in the gas phase.[16,17] For such transitions as N2 1s → π^*_{CN} we expect a sharp peak as for example in the N K-edge EELS spectrum of gaseous formamide, where a strong feature was attributed to the transition of the N 1s amide nitrogen to a π^* orbital.[41]

Our calculations assign the two broad features in the N K-edge NEXAFS spectrum of Gly-Gly at 405.70 and 407.35 eV to N1 1s → σ^*_{NC}, σ^*_{NH} and N2 1s → σ^*_{NC} transitions, respectively. This is in agreement with the published EELS spectrum of Gly-Gly in the gas phase.[16]

The O K-edge spectra of Gly-Gly are shown in Figure 6c, while in the inset the low-energy part of the Gly-Gly and Gly spectra are compared. The energies of the features in the Gly-Gly spectrum and proposed assignments are summarized in Table 3 (for assignments of the Gly spectrum, see ref 29). The two prominent peaks in the Gly spectrum are centered at 532.2 and 535.4 eV. The first feature is due to transition of 1s electrons of oxo O1 to $\pi^*_{C=O}$, while the transitions of 1s electrons of hydroxy O2 to π^*_{OC} and 3s/σ^*_{OH} contribute to the second strong peak. The difference of the Gly-Gly and Gly O K-edge spectra showed a peak at 531.85 eV, which is assigned to the O3 1s transition to the $\pi^*_{C=O}$ vacant orbital. This assignment is supported by studies of formamide and formic acid in the gas phase where the transitions of O 1s electrons to the $\pi^*_{C=O}$ orbital were observed at 531.5 and 532.1 eV, respectively.[41] The weak shoulder at lower energy (~530.9 eV) is due to O_2 in the residual gas (low 10^{-8} mbar) in the chamber, and the energy is in agreement with the previously published O K-edge NEXAFS spectrum of O_2.[45]

The difference in term values of the O3 1s → $\pi^*_{C=O}$ and O1 1s → $\pi^*_{C=O}$ transitions at the O K-edge of Gly-Gly is 0.9 eV, and it is consistent with the C K-edge spectrum, where transition of the C3 1s electron to the $\pi^*_{C=O}$ orbital had a lower term value than the C1 1s → $\pi^*_{C=O}$ transition (see Table 3).

The second strong peak in the O K-edge NEXAFS spectrum of Gly-Gly is mainly due to O2 1s → σ^*_{OC} and O2 1s → π^*_{OC} transitions, as in the corresponding peak of Gly. It is broader and more asymmetric than in Gly.

The O2 1s → 3p transition at 537.1 eV in the Gly-Gly spectrum (see Figure 6c) has been observed by us in spectra of other amino acids,[31,39,40] and it is interesting to note that this peak shifts by 0.9 eV to lower energy and is weaker compared with that of formic acid.[46] The broad structures at 539.5 and 542.5 eV observed in the spectra of Gly-Gly correspond to σ^* resonances associated with the O−H and C−OH single bonds.[16]

4. Conclusions

In this comparative study of the valence band, XPS, and NEXAFS spectra of glycine and glycyl-glycine, the features characteristic of peptide bond formation were identified and assigned by ab initio calculations. In the outer valence energy region of the Gly-Gly spectrum, new bands at 10.05 and 10.6 eV have been observed and they were related to the ionization of n_O and π_2 orbitals in the peptide group, and as well the inner valence part of C 2s bands showed additional peaks compared with the Gly spectrum. The C, N, and O 1s core level spectra of Gly-Gly were quantitatively fitted and assigned based on our calculation. In the O 1s photoemission spectrum, a chemical shift of 1.25 eV was observed between the oxo oxygen atoms of the carboxylic and peptide groups. In the C and O K-edge NEXAFS spectra the transition due to the 1s electron of peptide carbon and oxygen atoms to the $\pi^*_{C=O}$ vacant orbital was observed at lower energy compared with the transition of 1s electron of corresponding atoms in carboxylic group. Because of the internal hydrogen bonding between NH_2 and NH groups in the most populated *2t* Gly-Gly conformer, the resonance associated with the N1 1s → π^*_{CN} transition shifts with respect to Gly by ~0.6 eV to lower photon energy, while the resonance due to the N2 1s → π^*_{CN} transition contributes to the sharp peak at 402.3 eV.

Acknowledgment. O.P. acknowledges financial support from the Central European Initiative. We thank our colleagues at Elettra for their assistance, and for providing high-quality synchrotron light.

References and Notes

(1) de Vries, M. S.; Hobza, P. *Annu. Rev. Phys. Chem.* **2007**, *58*, 585.
(2) Klasinc, L. *J. Electron Spectrosc. Relat. Phenom.* **1976**, *8*, 16.

(3) Cannington, P. H.; Ham, N. S. *J. Electron Spectrosc. Relat. Phenom.* **1979**, *15*, 79.
(4) Cannington, P. H.; Ham, N. S. *J. Electron Spectrosc. Relat. Phenom.* **1983**, *32*, 139.
(5) Löfgren, P.; Krozer, A.; Lausmaa, J.; Kasemo, B. *Surf. Sci.* **1997**, *370*, 377.
(6) Hasselström, J.; Karis, O.; Weinelt, M.; Wassdahl, N.; Nilsson, A.; Nyberg, M.; Pettersson, L. G. M.; Samant, M. G.; Stöhr, J. *Surf. Sci.* **1998**, *407*, 221.
(7) Toomes, R. L.; Kang, J. H.; Woodruff, D. P.; Polcik, M.; Kittel, M.; Hoeft, J. T. *Surf. Sci.* **2003**, *522*, L9.
(8) Kang, J. H.; Toomes, R. L.; Polcik, M.; Kittel, M.; Hoeft, J. T.; Efstathiou, V.; Woodruff, D. P.; Bradshaw, A. M. *J. Phys. Chem.* **2003**, *118*, 6059.
(9) Barlow, S. M.; Raval, R. *Surf. Sci. Rep.* **2003**, *50*, 201.
(10) Messer, B. M.; Cappa, C. D.; Smith, J. D.; Wilson, K. R.; Gilles, M. K.; Cohen, R. C.; Saykally, R. J. *J. Phys. Chem. B* **2005**, *109*, 5375.
(11) Messer, B. M.; Cappa, C. D.; Smith, J. D.; Drisdell, W. S.; Schwartz, C. P.; Cohen, R. C.; Saykally, R. J. *J. Phys. Chem. B* **2005**, *109*, 21640.
(12) Slaughter, A. R.; Banna, M. S. *J. Phys. Chem.* **1988**, *92*, 2165.
(13) Plekan, O.; Feyer, V.; Richter, R.; Coreno, M.; de Simone, M.; Prince, K. C.; Carravetta, V. *Chem. Phys. Lett.* **2007**, *442*, 429.
(14) Plekan, O.; Feyer, V.; Richter, R.; Coreno, M.; de Simone, M.; Prince, K. C.; Carravetta, V. *J. Phys. Chem. A* **2007**, *111*, 10998.
(15) Richer, G.; Sandorfy, C. *J. Electron Spectrosc. Relat. Phenom.* **1984**, *34*, 327.
(16) Gordon, M. L.; Cooper, G.; Morin, C.; Araki, T.; Turci, C. C.; Kaznatcheev, K.; Hitchcock, A. P. *J. Phys. Chem. A* **2003**, *107*, 6144.
(17) Cooper, G.; Gordon, M.; Tulumello, D.; Turci, C.; Kaznatcheev, K.; Hitchcock, A. P. *J. Electron Spectrosc. Relat. Phenom.* **2004**, *137*−*140*, 795.
(18) Zubavichus, Y.; Zharnikov, M.; Schaporenko, A.; Grunze, M. *J. Electron Spectrosc. Relat. Phenom.* **2004**, *134*, 25.
(19) Chatterjee, A.; Zhao, L.; Zhang, L.; Pradhan, D.; Zhou, X.; Leung, K. T. *J. Chem. Phys.* **2008**, *129*, 105104.
(20) Prince, K. C.; Blyth, R. R.; Delaunay, R.; Zitnik, M.; Krempasky, J.; Slezak, J.; Camilloni, R.; Avaldi, L.; Coreno, M.; Stefani, Gly.; Furlani, C.; de Simone, M.; Stranges, S. *J. Synchrotron Radiat.* **1998**, *5*, 565.
(21) Kimura, K.; Katsumata, S.; Achiba, Y.; Yamazaki, T.; Iwata, S. *Handbook of He (I) Photoelectron Spectra of Fundamental Organic Molecules*; Japan Scientific Societies Press: Tokyo, Japan, 1981.
(22) Myrseth, V.; Bozek, J. D.; Kukk, E.; Sæthre, L. J.; Thomas, T. D. *J. Electron Spectrosc. Relat. Phenom.* **2002**, *122*, 57.
(23) Thomas, T. D.; Shaw, R. W., Jr. *J. Electron Spectrosc. Relat. Phenom.* **1974**, *5*, 1081.
(24) Hatamoto, T.; Matsumoto, M.; Liu, X.-J.; Ueda, K.; Hoshino, M.; Nakagawa, K.; Tanaka, T.; Tanaka, H.; Ehara, M.; Tamaki, R.; Nakatsuji, H. *J. Electron Spectrosc. Relat. Phenom.* **2007**, *155*, 54.
(25) Tronc, M.; King, Gly. C.; Read, F. H. *J. Phys. B: At. Mol. Phys.* **1979**, *12*, 137. *J. Phys. B: At. Mol. Phys.* **1980**, *13*, 999.
(26) Sodhi, R. N. S.; Brion, C. E. *J. Electron Spectrosc. Relat. Phenom.* **1984**, *34*, 363.
(27) Wight, G. R.; Brion, C. E. *J. Electron Spectrosc. Relat. Phenom.* **1974**, *3*, 191.
(28) DALTON, a molecular electronic structure program, Release 2.0, 2005, see http://www.kjemi.uio.no/software/dalton/dalton.html.
(29) Schafer, A.; Horn, H.; Ahlrichs, R. *J. Chem. Phys.* **1992**, *97*, 2571.
(30) Ågren, H.; Carravetta, V.; Vahtras, O.; Pettersson, L. G. M. *Theor. Chim. Acc.* **1997**, *97*, 14.
(31) Plekan, O.; Feyer, V.; Richter, R.; Coreno, M.; de Simone, M.; Prince, K. C.; Carravetta, V. *J. Electron Spectrosc. Relat. Phenom.* **2007**, *155*, 47.
(32) Ke, H.-W.; Rao, L.; Xu, X.; Yan, Y.-J. J. *Theor. Comput. Chem.* **2008**, *7*, 889.
(33) Csaszar, A. G. *J. Am. Chem. Soc.* **1992**, *114*, 9568.
(34) Gil, A.; Bertran, J.; Sodupea, M. *J. Chem. Phys.* **2006**, *124*, 154306.
(35) Schmidt, M. W.; Baldridge, K. K.; Boatz, J. A.; Elbert, S. T.; Gordon, M. S.; Jensen, J. J.; Koscki, S.; Matsunaga, N.; Nguyen, K. A.; Su, S.; Windus, T. L.; Dupuis, M.; Montgomery, J. A. *J. Comput. Chem.* **1993**, *14*, 1347.
(36) Falzon, C. T.; Wang, F.; Pang, W. *J. Phys. Chem. B* **2006**, *110*, 9713.
(37) Abu-samha, M.; Børve, K. J.; Sæthre, L. J.; Thomas, T. D. *Phys. Rev. Lett.* **2005**, *95*, 103002.
(38) Thomas, T. D.; Sæ´thre, L. J.; Børve, K. J. *Phys. Chem. Chem. Phys.* **2007**, *9*, 719.
(39) Feyer, V.; Plekan, O.; Richter, R.; Coreno, M.; Prince, K. C.; Carravetta, V. *J. Phys. Chem. A* **2008**, *112*, 7806.
(40) Zhang, W.; Carravetta, V.; Plekan, O.; Feyer, V.; Richter, R.; Coreno, M.; Prince, K. C. *J. Chem. Phys.* **2009**, *131*, 035103.
(41) Ishii, I.; Hitchcock, A. P. *J. Chem. Phys.* **1987**, *87*, 830.
(42) Kaznacheyev, K.; Osanna, A.; Jacobsen, C.; Plashkevych, O.; Vahtras, O.; Ågren, H.; Carravetta, V.; Hitchcock, A. P. *J. Phys. Chem. A* **2002**, *106*, 3153.
(43) Zubavichus, Y.; Schaporenko, A.; Grunze, M.; Zharnikov, M. *J. Phys. Chem. B* **2006**, *110*, 3420.
(44) Otero, E.; Urquhart, S. G. *J. Phys. Chem. A* **2006**, *110*, 12121.
(45) Coreno, M.; de Simone, M.; Prince, K. C.; Richter, R.; Vondráček, M.; Avaldi, L.; Camilloni, R. *Chem. Phys. Lett.* **1999**, *306*, 269.
(46) Prince, K. C.; Richter, R.; de Simone, M.; Coreno, M. *J. Phys. Chem. A* **2003**, *107*, 1955.

JP906843J